

## Quantitative Kinetic Analysis of Hydrogen Transfer Reactions from Dietary Polyphenols to the DPPH Radical

PASCALE GOUPY, CLAIRE DUFOUR, MICHELE LOONIS, AND OLIVIER DANGLES\*

UMR A 408 INRA-Université d'Avignon, Site Agroparc, Domaine St-Paul,  
 84914 Avignon Cedex 9, France

Diphenylpicrylhydrazyl (DPPH) is widely used for quickly assessing the ability of polyphenols to transfer labile H atoms to radicals, a likely mechanism of antioxidant protection. This popular test generally pays no attention to the kinetics of H atom transfer, which however could be even more important than the total H-atom-donating capacities (stoichiometry, EC<sub>50</sub>) typically evaluated. In the present work, a series of dietary polyphenols belonging to the most representative families (flavonols from onion, flavanol monomers and oligomers from barley, and caffeic acid and caffeoyl esters from artichoke and endive) are characterized not only by their total stoichiometries ( $n_{\text{tot}}$ ) but also by their rate constants of first H atom abstraction by DPPH ( $k_1$ ), deduced from the kinetic analysis of the decay of the DPPH visible band following addition of the antioxidant. The mildly reactive DPPH radical allows a good discrimination between polyphenols, as demonstrated by the relatively large ranges of  $k_1$  (ca. 400–5000 M<sup>-1</sup> s<sup>-1</sup>) and  $n_{\text{tot}}$  (ca. 1–5) values typically measured with antioxidants having a single polyphenolic nucleus. With antioxidants displaying more than one polyphenolic nucleus (procyanidin oligomers, dicaffeoyl esters), the kinetic analysis makes it possible to demonstrate significant differences in reactivity between the subunits (two distinct  $k_1$  values whose ratio lies in the range 3–10) and nonadditive stoichiometries.

**KEYWORDS:** Polyphenol; flavonol; flavanol; procyanidin; caffeic acid ester; antioxidant; DPPH; kinetics

### INTRODUCTION

The benefits of a diet rich in plant products (fruits, vegetables, tea, red wine) are well evidenced from epidemiological studies, especially concerning the prevention of cardiovascular diseases (CVD) and cancers. Being the most ubiquitous food microconstituents, plant polyphenols probably play an important role in these protective effects (1, 2). Since reactive oxygen species (ROS) may be involved in the development of CVD and cancers, their efficient trapping by polyphenols (3–14) is one of the likely mechanisms by which these antioxidants may act. After a meal rich in plant products, low concentrations (0.1–1 μM) of dietary polyphenols (e.g., flavonols) can be detected in plasma as serum albumin-bound conjugates (sulfates, glucuronides) (2, 15–17). These circulating forms could protect low-density lipoproteins (LDL, the main targets of oxidative stress in plasma) by directly reacting with ROS and also by regenerating LDL-bound α-tocopherol. Moreover, the much more abundant nonabsorbed dietary polyphenols (e.g., oligomeric procyanidins) could also inhibit oxidative stress directly in the gastrointestinal tract (18, 19).

Many in vitro studies have addressed the antioxidant properties of polyphenols (3–14), and reasonably consistent structure–

activity relationships have been published concerning the inhibition of lipid peroxidation and the trapping of ROS and colored radicals. In particular, diphenylpicrylhydrazyl (DPPH, **Figure 1**) is widely used for quickly assessing the ability of antioxidants to transfer labile H atoms to radicals (20, 21). In the DPPH test, antioxidants are typically characterized by their EC<sub>50</sub> value (concentration necessary to reduce 50% of DPPH) or their stoichiometry (number of DPPH molecules reduced by one molecule of antioxidant). As an extension of previous investigations by our group (22–25), the present work is aimed at showing that a detailed kinetic analysis of the decay in the DPPH absorption band that follows the addition of the antioxidant provides additional interesting information about the mechanisms of H atom donation and the relative reactivities of distinct antioxidant subunits.

In this work, a series of dietary polyphenols belonging to the most representative families were investigated: flavonols from onion, flavanol monomers and oligomers (procyanidins or condensed tannins) from barley, and caffeic acid and caffeoyl esters from artichoke and endive (**Figure 1**).

### MATERIALS AND METHODS

**Chemicals.** Methanol, acetone, ethyl acetate, and acetonitrile were of HPLC grade (Carlo Erba). Petroleum ether was of analytical reagent

\* To whom correspondence should be addressed [telephone (33) 490 14 44 32; fax (33) 490 14 44 41; E-mail Olivier.Dangles@univ-avignon.fr].

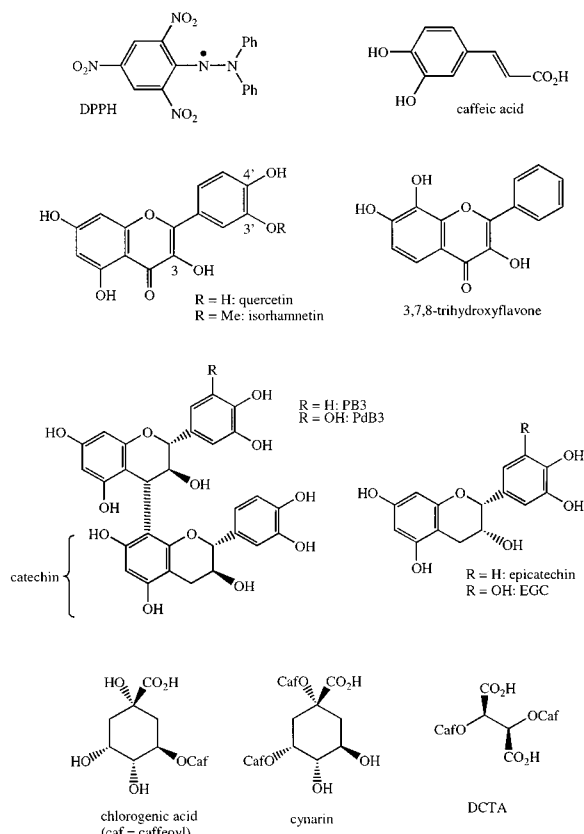


Figure 1. Chemical structures of the polyphenols investigated.

grade from SDS. Quercetin, isoquercitrin (quercetin-3-*O*- $\beta$ -D-glucoside), isorhamnetin (3'-*O*-methylquercetin), and cynarin (1,5-dicaffeoylquinic acid) were obtained from Extrasynthese (Genay, France). Caffeic acid, chlorogenic acid (3-caffeoylquinic acid), catechin, epicatechin, epigallocatechin (EGC), and 1,1-diphenyl-2-picrylhydrazyl (DPPH) were obtained from Sigma. 3,7,8-Trihydroxyflavone [chemically synthesized according to ref (26)] was a generous gift from Prof. R. Brouillard (University of Strasbourg, France). Barley flavanols were extracted, purified, and analyzed according to the literature (21).

**Extraction and Purification of Flavonols from Onion.** A 50-g sample of fresh onions slices was blended with 200 mL of cold methanol using a domestic food processor at room temperature for 2 min, homogenized for 1 min using an Ultra-Turrax blender, and centrifuged at 4 °C at 10 000 rpm for 20 min. The supernatant was filtered on Whatman paper. Two successive extractions of the pellet were carried out after trituration for 1 min with 200 mL of cold methanol. The three filtrates were joined and concentrated to a volume of 500 mL under vacuum at 35 °C. The extract was filtered through an Acrodisc filter (0.22  $\mu$ m) before HPLC analysis. The flavonol extracts were stored at -20 °C until use.

Flavonol extracts were purified using a column (200  $\times$  26 mm) filled with 100 mL of SP700 resin, previously washed with water. Flavonol extracts (250 mL) were concentrated to dryness under vacuum at 35 °C, and the residue was dissolved in 50 mL of bidistilled water. The resin was loaded with this extract and washed with 500 mL of bidistilled water at a flow rate of 50 mL h<sup>-1</sup>. Flavonols were eluted with methanol. The methanolic fractions were concentrated to a volume of 50 mL under vacuum at 35 °C.

Quercetin-3,4'-di- $\beta$ -D-glucoside (QDG), quercetin-4'- $\beta$ -D-glucoside (QG), and isorhamnetin-4'- $\beta$ -D-glucoside (IG) were purified by fractionation on a column (450  $\times$  50 mm) filled with Fractogel Toyopearl HW-40(s) (TOSOH, Merck). Fractionation was carried out with methanol at a flow rate of 125 mL h<sup>-1</sup> (UV detection at 360 nm). After concentration under vacuum at 35 °C, the fractions containing QG, QDG, and IG were lyophilized and stored at -20 °C until use.

**Extraction and Purification of Polyphenols from Endive and Artichoke.** Samples of 5 g of endive leaves or 7 g of artichoke leaves

(lyophilized powder) were homogenized in 250 mL of ethanol-H<sub>2</sub>O (4:1) containing 0.5% sodium metabisulfite. Three successive extractions with ethanol-H<sub>2</sub>O (4:1) were carried out at 4 °C for 30 min. After elimination of ethanol under vacuum at 35 °C, ammonium sulfate (20%) and metaphosphoric acid (2%) were added to the aqueous phase. After removal of pigments and most of the lipids by three successive extractions with petroleum ether (2:1), the polyphenols were extracted with ethyl acetate (1:1) three times. The three organic phases were combined, filtered on Whatman paper, and concentrated to dryness under vacuum at 35 °C. The residue was dissolved in 3 mL of MeOH. The methanolic extract was filtered through Acrodisc filter (0.45  $\mu$ m) before HPLC analysis.

(*R,R*)-Dicafeoyltartaric (chicoric) acid (DCTA) was purified by fractionation of the endive methanolic extracts on a column (720  $\times$  26 mm) filled with LH20 (Sigma). Elution was carried out with 96% ethanol at a flow rate of 22 mL h<sup>-1</sup> (UV detection at 280 nm). Dicafeoyl quinic acids (DCQA1, DCQA2) were purified by fractionation of the artichoke methanolic extracts under essentially the same conditions (flow rate, 30 mL h<sup>-1</sup>). After concentration under vacuum at 35 °C, the fractions were lyophilized and stored at -20 °C until use.

**HPLC Analysis.** HPLC analyses of polyphenols were performed by RP-HPLC coupled to diode array detection (Hewlett-Packard 1100 or 1050) using an Alltima C18 column (5  $\mu$ m, 150  $\times$  4.6 mm) equipped with an Alltima C18 guard column (5  $\mu$ m, Alltech) (flow rate, 1 mL min<sup>-1</sup>; *T* = 35 °C; volume injected, 10  $\mu$ L). The solvent system used for flavonols was a gradient of A (0.05% HCOOH in H<sub>2</sub>O) and B (CH<sub>3</sub>CN) with 10% B at 0 min and 40% B at 40 min. The solvent system used for DCTA was a gradient of A (0.05% HCOOH in H<sub>2</sub>O) and B (CH<sub>3</sub>CN/MeOH/H<sub>2</sub>O, 3:1:1) with 5% B at 0 min, 10% B at 20 min, 25% B at 30 min, 25% B at 55 min, 30% B at 65 min, 50% B at 75 min, 50% B at 85 min, and 100% B at 100 min. A gradient of B and CH<sub>3</sub>CN was then applied with 50% B and 50% CH<sub>3</sub>CN at 120 min and 100% CH<sub>3</sub>CN at 125 min until 140 min. The solvent system used for DCQA1 and DCQA2 (*T* = 20 °C) was a gradient of A (0.05% HCOOH in H<sub>2</sub>O) and B (CH<sub>3</sub>CN) with 10% B at 0 min, 10% B at 8 min, 17% B at 15 min until 22 min, 18% B at 25 min until 30 min, 30% B at 40 min. Each polyphenol was identified by its retention time and UV-visible spectrum after comparison with the literature (27–29). Both DCQA1 and DCQA2 were structurally different from cynarin (1,5-dicaffeoylquinic acid). In addition to cynarin, 3,5-dicaffeoylquinic acid and, to a lesser degree, 1,4- and 4,5-dicaffeoylquinic acids have been identified in artichoke (28).

**HPLC/MS Analysis.** Polyphenol identification was confirmed by HPLC/MS (Platform LCZ, Micromass coupled to a HP 1050 HPLC system; see HPLC Analysis for the conditions of elution) or direct mass analysis (infusion) in the negative electrospray ionization mode (nitrogen flow, 500 L h<sup>-1</sup>; source and desolvation temperature, 100 and 300 °C, respectively; flow rate into the source, 50  $\mu$ L min<sup>-1</sup>). The following figures in parentheses refer to the voltages (in volts) of the capillary, sample cone, and extraction cone, respectively, used for analyzing the different polyphenols: onion flavonols (-3000, -30, -7), barley flavanols (-3000, -30, -5), DCTA (-3500, -40, -5), DCQA (-2500, -20, -14).

**H Atom Abstraction by DPPH.** The H-transfer reactions from an antioxidant to DPPH were monitored using a HP 8453 diode array spectrometer equipped with a magnetically stirred quartz cell (optical path length, 1 cm). The temperature in the cell was kept at 25 °C by means of a thermostated bath. Typical procedure: to 2 mL of a freshly prepared 2  $\times$  10<sup>-4</sup> M solution of DPPH in methanol, placed in the spectrometer cell, were added 25–125  $\mu$ L of a freshly prepared 10<sup>-3</sup> M solution of the antioxidant in the same solvent. Spectra were recorded every 0.5 s over 1–2 min for the determination of rate constants and stoichiometries. Kinetic runs over 15 min were used for the determination of total stoichiometries (see text for details).

**Data Analysis.** The curve-fittings of the absorbance vs time plots were carried out on a Pentium PC using the Scientist program (MicroMath, Salt Lake City, UT). Lambert and Beer's law and sets of differential kinetic equations (see text for the kinetic models used) with initial conditions on concentrations were input in the model. Curve-fittings were achieved through least-squares regression and yielded optimized values for the parameters (kinetic rate constants, stoichiom-

eries). Values reported in the tables for a given antioxidant at a given DPPH–antioxidant molar ratio are means of three experiments for the rate constants and stoichiometry  $n$  (fast step) and of two experiments for the total stoichiometry  $n_{\text{tot}}$ . Standard deviations are reported. The curve-fitting procedures typically gave good ( $>0.99$ ) to excellent ( $>0.999$ ) correlation coefficients. Consequently, the standard deviations due to the curve-fittings were low and were not taken into account.

## RESULTS AND DISCUSSION

The H-transfer reactions from polyphenols to DPPH were monitored by UV/vis spectroscopy by recording the decay of the DPPH visible absorbance ( $\lambda_{\text{max}} = 515$  nm in MeOH, molar absorption coefficient  $\epsilon = 11\,240$  M $^{-1}$  cm $^{-1}$  assuming a purity of 95%) that follows the addition of the antioxidant to the DPPH solution. The experiments (each one run in triplicate) were repeated with DPPH–antioxidant molar ratios typically ranging from 3 to 16 in order to exhaust the H-donating ability of the antioxidant. The higher values ( $>10$ ) were only considered with the antioxidants of highest stoichiometry, especially the ones having several distinct polyphenolic nuclei (e.g., procyanidins).

With potent antioxidants, the visible absorbance quickly decays over 1–2 min as a result of the transfer of the most labile H atoms of the antioxidant (fast step). This step is typically followed by a much slower decrease of the visible absorbance, featuring the residual H-donating ability of the antioxidant degradation products (slow step) (22–25). Only the fast steps were subjected to a detailed kinetic analysis. However, experiments extending over 15 min were used for the determination of the total stoichiometry ( $n_{\text{tot}}$ ) of the antioxidant using eq 1 ( $A_f$ , final visible absorbance;  $A_0$ , initial absorbance;  $c$ , initial

$$n_{\text{tot}} = \frac{A_0 - A_f}{\epsilon c} \quad (1)$$

antioxidant concentration) (Table 1). Of course, the initial DPPH–antioxidant molar ratio  $A_0/\epsilon c$  must be higher than  $n_{\text{tot}}$  for eq 1 to apply.

**General Kinetic Model (Model 1).** Different kinetic models were used for analyzing the H-atom-transfer reaction between DPPH and a given antioxidant during the fast step (1–2 min). The most simple (model 1) makes no hypothesis about the mechanism of antioxidant degradation. An antioxidant of stoichiometry  $n$  is simply regarded as  $n$  independent antioxidant subunits, AH, which all transfer a single H atom to DPPH with the same second-order rate constant  $k$  (22–24). Hence, eqs 2 and 3 can be used in the curve-fitting of the absorbance vs time

$$A = \epsilon[\text{DPPH}] \quad (2)$$

$$R = -\frac{d}{dt}[\text{AH}] = -\frac{d}{dt}[\text{DPPH}] = k[\text{AH}][\text{DPPH}] \quad (3)$$

plots ( $A$ , visible absorbance at time  $t$ ;  $A_0$ , initial absorbance;  $c$ , initial antioxidant concentration;  $c_0$ , initial DPPH concentration;  $C$ , initial concentration of antioxidant subunit AH;  $C = nc$ ).

The initial rate of DPPH consumption may be written as  $R_0 = kncc_0 = k_1cc_0$ ,  $k_1$  being the rate constant for the first H atom abstraction from the antioxidant. Hence,  $k$  can be identified with  $k_1/n$ . In this work, the curve-fittings using model 1 were carried out with  $n$  and  $k_1$  as the floating parameters, since  $k_1$  allows a more straightforward comparison between antioxidants than  $k$ .

The estimation of  $n$  and  $k_1$  can be carried out simply, even when software able to deal with differential equations is not available. On one hand,  $n$  can be estimated by using eq 1, with  $A_f$  now standing for the visible absorbance at the end of the

**Table 1.** Abstraction of H Atoms from Polyphenols by DPPH (MeOH, 25 °C): Total Stoichiometries  $n_{\text{tot}}$  Calculated from Eq 1 after 15 min of Reaction

DPPH/antioxidant molar ratio	caffeic acid	chlorogenic acid	cynarin
10.8–11.3	2.65 ± 0.03	2.43 ± 0.04	4.10 ± 0.06
7.5–7.9	2.65 ± 0.01	2.41 ± 0.01	3.98 ± 0.03
5.4–5.6	2.67 ± 0.05	2.40 ± 0.01	3.98 ± 0.08

DPPH/antioxidant molar ratio	DCQA1	DCQA2	DCTA <sup>a</sup>
9.4–11.6	3.50 ± 0.01	3.13 ± 0.01	3.77 ± 0.04
6.6–8.2	3.39 ± 0.16	3.15 ± 0.03	3.60 ± 0.01
4.8–5.8	3.51 ± 0.03	3.10 ± 0.03	2.94 ± 0.01

DPPH/antioxidant molar ratio	catechin	epicatechin	EGC
10.7–11.6	3.72 ± 0.02	3.96 ± 0.05	3.94 ± 0.05
7.4–8.2	3.43 ± 0.03	3.42 ± 0.02	3.63 ± 0.01
5.3–5.7	3.25 ± 0.01	3.23 ± 0.03	3.38 ± 0.01

DPPH/antioxidant molar ratio	PC2	PB3	PdB3
17–21	9.35 ± 0.03	6.47 ± 0.13	7.08 ± 0.05
14.6–16.5	8.72 ± 0.05	6.35 ± 0.01	6.55 ± 0.07
10.5–12.0	8.68 ± 0.03	6.31 ± 0.03	6.15 ± 0.01

DPPH/antioxidant molar ratio	quercetin	isoquercitrin	isorhamnetin
10.8–11.0	4.86 ± 0.12	3.78 ± 0.08	
7.6–7.7	4.69 ± 0.01	3.69 ± 0.02	2.38 ± 0.02
5.3–5.4		3.47 ± 0.04	2.32 ± 0.01

DPPH/antioxidant molar ratio	QG	QDG	IG
5.2–5.5	1.22 ± 0.04	0.40 ± 0.01	0.93 ± 0.03
3.7–3.9	1.22 ± 0.01	0.38 ± 0.01	0.91 ± 0.02
2.9–3.3	1.18 ± 0.01	0.36 ± 0.01	0.87 ± 0.01

<sup>a</sup>DCTA, slow decay, reaction not completed after 15 min. For 3,7,8-trihydroxyflavone, stoichiometries with DPPH/antioxidant molar ratios of 5.6, 3.9 and 3.1 are  $1.73 \pm 0.02$ ,  $1.66 \pm 0.01$ , and  $1.59 \pm 0.01$ , respectively.

fast step. On the other hand, eq 3 has to be integrated to yield eq 4. Thus, when  $\ln\{(1 - A_f/A)/(1 - A_f/A_0)\}$  is plotted as a

$$\ln \frac{1 - A_f/A}{1 - A_f/A_0} = -\frac{k_1 c}{A_0/A_f - 1} t \quad (4)$$

function of time, a straight line with zero intercept is obtained over most of the duration of the fast step (Figure 2), divergence occurring only when  $A$  gets close to  $A_f$ . The slope of the line readily gives access to  $k_1$ .

In the experiment concerning catechin shown in Figure 2, the corresponding  $n$  and  $k_1$  values ( $n = 2.18$ ,  $k_1 = 1008$  M $^{-1}$  s $^{-1}$ ,  $r = 0.999$ , lower plot) are in very good agreement with those deduced from the nonlinear regression using eqs 2 and 3 ( $n = 2.18 \pm 0.01$ ,  $k_1 = 1028 \pm 11$  M $^{-1}$  s $^{-1}$ ,  $r = 0.999$ , upper plot). It must be noted that the duration of the fast step, and consequently the  $n$  value, displays a somewhat arbitrary character since the visible absorbance typically keeps decaying over much longer periods, although much more slowly. Indeed, the duration of the fast step is determined by visual appreciation. In Figure 2, for instance, it is clear that most of the H-donating activity of catechin is dissipated within 50 s in our conditions. Hence,  $n$  gives only a crude estimate of the number of most

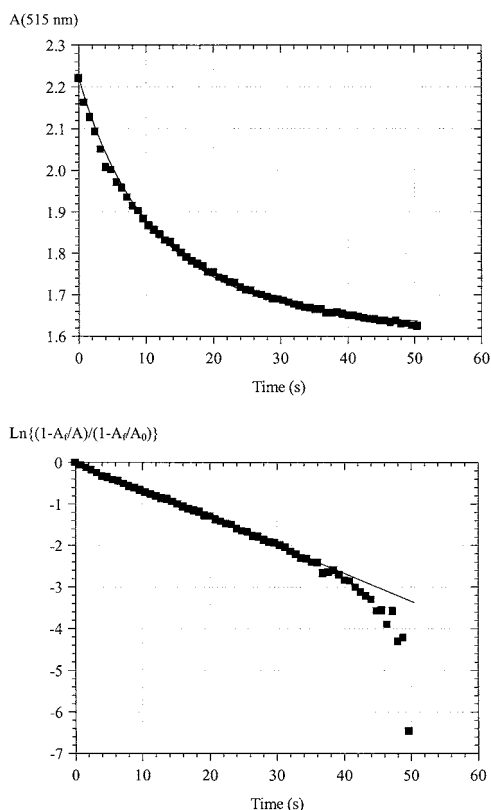


**Figure 2.** (Top) Decay of the visible absorbance (515 nm) of a DPPH ( $2 \times 10^{-4}$  M) solution in MeOH (25 °C) following addition of catechin ( $2.5 \times 10^{-5}$  M). (Bottom) Estimation of the rate constant for first H atom abstraction ( $k_1$ ) using eq 4. For details, see text.

labile H atoms transferred to DPPH. On the other hand, the  $k_1$  value is essentially independent of the time interval selected, since its determination rests on the early stage of the reaction. In summary, when the duration of the fast step is raised,  $n$  increases,  $k$  decreases, and  $k_1 = nk$  remains essentially constant. [In principle, the  $k_1$  value could be directly estimated under pseudo-first-order conditions with  $c \gg c_0$ . However, under such conditions, the decay of the DPPH absorption band becomes too fast to be accurately monitored by conventional UV–visible spectroscopy.]

Polyphenols displaying a free 1,2-dihydroxybenzene (catechol) ring typically give  $n$  values per catechol group close to 2 (Tables 2 and 3), in agreement with the stepwise formation of semiquinone radicals and quinones during the fast step. In the case of quercetin and EGC,  $n$  values close to 3 reflect the additional H-donating ability of C(3)–OH (quercetin) and C(5')–OH (EGC). Quinone intermediates have actually been clearly evidenced in the reaction of different 3',4'-dihydroxyflavonoids with DPPH (22, 23). In the case of isorhamnetin, the stepwise H abstraction at C(3)–OH and C(4')–OH allows  $p$ -quinonoid formation with a resulting stoichiometry of 2 (Figure 3). Hence, 3',4'-dihydroxy and 3,4'-dihydroxy substitutions in flavones and flavonols favor the H-donating activity in terms of both rate constants (radical stabilization) and relatively high stoichiometries (quinone and  $p$ -quinonoid formation). In the case of quercetin, the 3,3',4'-trihydroxy substitution has the additional advantage of allowing the regeneration of a catechol nucleus upon solvent addition at C(2). Hence, subsequent H abstractions by DPPH become possible, thus leading to higher total stoichiometries of 4–5. The corresponding  $p$ -quinonoid–solvent adducts have been characterized, not only in the

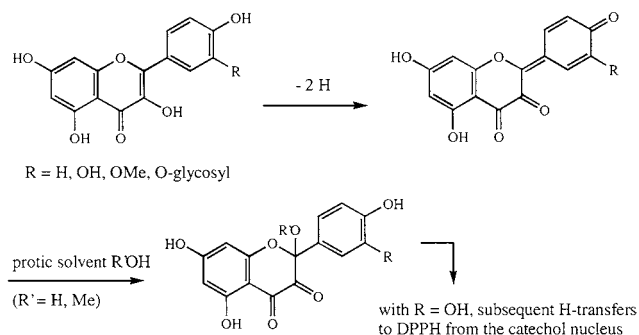


**Figure 3.** Proposed pathways of oxidative degradation of flavonols during radical capture in protic solvents.

quercetin–DPPH reaction (20) but also in a variety of chemical, electrochemical, and enzymatic reactions (30–35). Despite a catechol group and an expectedly high  $k_1$  value, 3,7,8-trihydroxyflavone displays relatively low  $n$  and  $n_{\text{tot}}$  values ( $<2$ ). In this case, the quinone initially formed may react with the residual parent flavone to form inert dimers. Since the stoichiometries of quinone formation and dimerization are respectively 2 ( $\text{AH}_2 + 2\text{DPPH} \rightarrow \text{A} + 2\text{DPPH-H}$ ) and 1 ( $2\text{AH}_2 + 2\text{DPPH} \rightarrow (\text{AH})_2 + 2\text{DPPH-H}$ ), this could actually result in the observed stoichiometry of ca. 1.5 at the end of the fast step. Similarly, caffeic acid and chlorogenic acid display total stoichiometries only slightly higher than the partial stoichiometries at the end of the fast step (ca. 2). Since caffeic acid is known to be quite prone to oxidative dimerization (36, 37), formation of inert, sterically hindered dimers may also limit the overall H-donating activity. Note that the difference in  $k_1$  values between caffeic acid and chlorogenic acid actually confirms that H abstraction by DPPH is sensitive to steric hindrance. Glycosidation at C(4')–OH of the flavone nucleus (QG, QDG, IG) markedly depresses the H-donating ability, with  $n_{\text{tot}}$  values of the order of 1 or lower (reactions not completed after 15 min, Table 1). In such situations, the aryloxy radicals probably quickly recombine into inert dimers.

As expected, procyanidin oligomers display stoichiometries that increase with the number of monomer units. However, the total stoichiometries are not strictly additive (Table 1). Thus,  $n_{\text{tot}}$  values per flavanol unit are 3.7 for catechin and 2.9–3.2 for PB3 and PC2. Similar observations were reported in the reaction of the ABTS radical cation with procyanidins (38). In addition, the  $k_1$  values for the oligomers are significantly lower than those for the corresponding monomer (Tables 2 and 3). These results suggest that monomer units within oligomers are not equally available for reaction with DPPH (steric hindrance). The nonadditivity of  $n_{\text{tot}}$  is even more obvious in the dicaffeoylquinic series. Thus, the total stoichiometries per caffeoyl unit are 2.4 for chlorogenic acid, 2.0 for cynarin, and 1.5–1.7 for the cynarin regioisomers DCQA1 and DCQA2. However, the  $k_1$  values are rather close within this series and eventually higher for DCQA1 and DCQA2 than for chlorogenic acid. Hence, it may be speculated that one caffeoyl unit out of two readily reacts with DPPH and that subsequent coupling reactions between the two caffeoyl units lock the antioxidant under nonreactive rigid structures, thus resulting in a loss in stoichiometry. Steric hindrance seems particularly critical when the two caffeoyl moieties are linked to the small tartaric acid core since DCTA only very slowly transfers its phenolic H atoms to DPPH. The nonadditivity of the antioxidant stoichiometries in the dicaffeoylquinic acids is in contrast with investigations on polygalloyl esters of sucrose (24). In the latter series, each



galloyl unit, even within the relatively hindered octagalloyl derivative, remains available to DPPH radicals, in agreement with additive stoichiometries and similar rate constants within the series.

In a second step, refined kinetic models were used to take into account the fate of the aryloxy radicals and the distinct reactivities of the different polyphenolic units of oligomeric procyanidins and dicaffeoylquinic acids.

**Polyphenols That Form Quinone or *p*-Quinonoid Intermediates (Model 2).** In the case of polyphenols having a single 1,2-dihydroxy substitution (except for 3,7,8-trihydroxyflavone), the semiquinone radicals (AH<sup>•</sup>) formed in the first step (rate constant  $k_1$ ) were assumed to quickly disproportionate to form the corresponding quinone (A) and regenerate the parent polyphenol (AH<sub>2</sub>). This is in agreement with the fast second-order decay of polyphenolic aryloxy radicals in water ( $2k$  in the range  $10^6$ – $10^8$  M<sup>-1</sup> s<sup>-1</sup>), evidenced by pulse radiolysis investigations (8, 37). Alternatively, the quinone could form upon direct H transfer from the semiquinone radical to DPPH. Although not documented, this reaction may take place in competition with semiquinone disproportionation. Including this step in our kinetic scheme is not expected to strongly affect the resulting  $k_1$  values but would markedly complicate the rate laws used in the curve-fittings. Hence, it has been neglected throughout this work. The quinone, or more probably its derivatives (solvent adducts, dimers, degradation products), may have a residual H-donating ability (rate constant  $k_2$ ). Assuming a quasi-stationary state for the radicals, eqs 5–7 were derived (22, 25) and used in the curve-fitting of the kinetic traces (model 2) to give optimized  $k_1$  and  $k_2$  values that are in reasonable agreement for different DPPH–antioxidant molar ratios (Table 2). In addition, models 1 and 2 give consistent values for  $k_1$ .

$$-\frac{d}{dt}[\text{DPPH}] = k_1[\text{AH}_2][\text{DPPH}] + k_2[\text{A}][\text{DPPH}] \quad (5)$$

$$-\frac{d}{dt}[\text{AH}_2] = \frac{k_1}{2}[\text{AH}_2][\text{DPPH}] \quad (6)$$

$$\frac{d}{dt}[\text{A}] = \frac{k_1}{2}[\text{AH}_2][\text{DPPH}] - k_2[\text{A}][\text{DPPH}] \quad (7)$$

In the case of quercetin, tautomerism in the *o*-quinone allows solvent addition on the C ring. The quinone–solvent adducts display a catechol nucleus (B ring) which, in turn, can enter a sequence of semiquinone formation and subsequent disproportionation ( $k_2/2$  in eq 7 in the place of  $k_2$ ). On the other hand, quinone formation in the catechin series is more probably followed by dimerization, since catechin dimers are readily produced under oxidative conditions including radical capture (21, 39, 40). Even though  $k_2$  is ill-defined because of the different fates of the *o*-quinone and/or *p*-quinonoid intermediates, its value is typically much lower than that of  $k_1$ . Hence, H abstraction from intermediates is much slower than that from the parent polyphenol.

**Polyphenols with Discriminated Antioxidant Subunits (Model 3).** In the case of oligomeric procyanidins and dicaffeoylquinic acids, model 2 was adapted to single out the most reactive monomer unit, subsequently referred to as the *external* unit, EH<sub>2</sub> (rate constant  $k_{1e}$  for abstraction of the first H atom). The other monomer unit (procyanidins B3, dicaffeoylquinic acids) or the two other ones (procyanidin C2) are considered as *internal* (IH<sub>2</sub>) and thus less available (rate constant  $k_{1i} < k_{1e}$ ).

Hence, eqs 5–7 are modified as follows (model 3):

$$-\frac{d}{dt}[\text{DPPH}] = k_{1e}[\text{EH}_2][\text{DPPH}] + k_{1i}[\text{IH}_2][\text{DPPH}] + k_2[\text{A}][\text{DPPH}] \quad (8)$$

$$-\frac{d}{dt}[\text{EH}_2] = \frac{k_{1e}}{2}[\text{EH}_2][\text{DPPH}] \quad (9)$$

$$-\frac{d}{dt}[\text{IH}_2] = \frac{k_{1i}}{2}[\text{IH}_2][\text{DPPH}] \quad (10)$$

$$\frac{d}{dt}[\text{A}] = \frac{k_{1e}}{2}[\text{EH}_2][\text{DPPH}] + \frac{k_{1i}}{2}[\text{IH}_2][\text{DPPH}] - k_2[\text{A}][\text{DPPH}] \quad (11)$$

In the curve-fittings, the initial concentrations of EH<sub>2</sub> and IH<sub>2</sub> are both  $c$  for PB3, PdB3, and the dicaffeoylquinic acids, and respectively  $c$  and  $2c$  for PC2,  $c$  being the total antioxidant concentration. For PC2, only one monomer could be shown to react faster, since the highest rate constant is associated with the unit in concentration  $c$ . The excellent correlation coefficients ( $\geq 0.999$ ) obtained when using model 3 outline the pertinence of a discrimination between the different antioxidant units in the analysis of the kinetic data. In the case of dimers PB3 and PdB3, the external unit is ca. 3–4 times as reactive as the internal one (Table 3), each external unit being roughly as reactive as the corresponding monomer (catechin or EGC). For PC2, the difference in reactivity ( $k_{1e}/k_{1i}$ ) reaches a factor of ca. 10. Recently, type B dimers have been shown to be converted into the corresponding type A dimers upon trapping of DPPH radicals (41) (Figure 4). The mechanism proposed involved nucleophilic attack of the C(7)–OH group of the lower unit on the C(2) center of a *p*-quinonoid intermediate derived from the upper unit. This mechanism is consistent with our kinetic data on B3 procyanidins and suggests that the upper unit could be more efficient in trapping DPPH radicals (rate constant  $k_{1e}$ ). However, the stoichiometry  $n$  is more than twice as large as the value of 2 that would be consistent with the sole dimer B–dimer A conversion. Hence, pathways involving H abstraction from intermediate type A dimers (contributing to rate constant  $k_2$ ) and H abstraction from the lower unit (rate constant  $k_{1i}$ ) must operate. Interestingly, discrimination between the two flavanol units may also take place in dimers A. Indeed, EPR measurements suggest that radical formation preferentially occurs in the upper unit of procyanidin A2 (42).

In the case of the dicaffeoylquinic acids (Table 3), the  $k_{1e}/k_{1i}$  ratio is close to 10 for DCQA1 and DCQA2 and ca. 4–5 for cynarin, which, despite its slightly higher stoichiometry, is less reactive (lower  $k_{1e}$  value) than DCQA1 and DCQA2. It must be noted that these distinct reactivities do not reflect differences in electron density between the monomer units or differences in radical stability but rather reflect differences in availability between the monomer units in the preferred conformations of the antioxidant. Interestingly, the conformational analysis of cynarin by NMR has shown that both caffeoyl moieties occupy axial positions on the quinic core (43). This parallel arrangement should favor stacking interactions between the flat cinnamic nuclei that may be responsible for one unit being shielded from the DPPH radical by the other. Such a conformation should also favor intramolecular coupling reactions between the caffeoyl moieties during radical capture.

**Polyphenols That Do Not Form Quinone or *p*-Quinonoid Intermediates (Model 4).** Finally, model 4 was used for the

**Table 2.** Abstraction of H Atoms from Polyphenols by DPPH (MeOH, 25 °C)<sup>a</sup>

anti-oxidant	DPPH/antioxidant molar ratio (kinetic model)	$k_1$ (M <sup>-1</sup> s <sup>-1</sup> )	$k_2$ (M <sup>-1</sup> s <sup>-1</sup> )	$n$
catechin	8 (2)	1037 ± 38	28 ± 6	
	8 (1)	1005 ± 41		2.15 ± 0.03
	11.4 (2)	1123 ± 42	35 ± 13	
	11.4 (1)	1071 ± 38		2.19 ± 0.09
	16 (2)	1172 ± 105	29 ± 18	
epicatechin	16 (1)	1120 ± 86		2.15 ± 0.13
	8 (2)	1165 ± 84	40 ± 5	
	8 (1)	1019 ± 75		2.30 ± 0.04
	11.4 (2)	1124 ± 64	48 ± 13	
EGC	11.4 (1)	944 ± 77		2.34 ± 0.13
	16 (2)	1272 ± 105	33 ± 14	
	16 (1)	1224 ± 111		2.16 ± 0.09
	5.7 (1)	3899 ± 276		3.04 ± 0.03
caffeic acid	8 (1)	4926 ± 311		3.04 ± 0.01
	11.4 (1)	5455 ± 376		3.00 ± 0.04
	5.7 (2)	1275 ± 38	42 ± 0	
chlorogenic acid	5.7 (1)	1178 ± 52		2.24 ± 0.04
	8 (2)	1285 ± 104		
	8 (1)	1304 ± 65		1.99 ± 0.06
	5.7 (2)	373 ± 5	15 ± 1	
quercetin <sup>b</sup>	5.7 (1)	363 ± 4	15 ± 1	
	8 (2)	522 ± 18		2.19 ± 0.02
	8 (1)	507 ± 23		2.16 ± 0.01
	4 (2)	1907 ± 56	273 ± 8	
	4 (1)	1536 ± 29		3.10 ± 0.08
	5.7 (2)	1993 ± 24	227 ± 19	
	5.7 (1)	1647 ± 32		2.90 ± 0.05
isorhamnetin	8 (2)	2252 ± 63	179 ± 17	
	8 (1)	1729 ± 29		2.81 ± 0.09
	11.4 (2)	2381 ± 86	191 ± 21	
	11.4 (1)	1694 ± 49		2.91 ± 0.11
	3.2 (2)	1973 ± 24	109 ± 19	
	3.2 (1)	1840 ± 33		2.33 ± 0.05
	4 (2)	1995 ± 64	55 ± 3	
isoquercitrin	4 (1)	1863 ± 51		2.20 ± 0.01
	5.7 (2)	1975 ± 59	22 ± 9	
	5.7 (1)	1902 ± 24		2.09 ± 0.04
	8 (2)	2063 ± 17	36 ± 13	
	8 (1)	1863 ± 86		2.13 ± 0.09
	3.2 (2)	1187 ± 14		
	3.2 (1)	1176 ± 28		2.03 ± 0.07
	4 (2)	1311 ± 69		
3,7,8-trihydroxyflavone	4 (1)	1318 ± 13		2.02 ± 0.06
	5.7 (2)	1441 ± 104		
	5.7 (1)	1534 ± 17		1.95 ± 0.07
	8 (2)	1563 ± 106		
	8 (1)	1677 ± 101		1.95 ± 0.12

<sup>a</sup> Rate constants calculated from the curve-fitting of the absorbance (515 nm) vs time plots according to model 1 ( $k_1$ ,  $n$ ) or model 2 ( $k_1$ ,  $k_2$ ). For details, see text.

<sup>b</sup> Two sequences of quinone formation with intermediate fast solvent addition ( $k_2/2$  instead of  $k_2$  in model 2).

kinetic analysis of poorly reactive antioxidants, i.e., antioxidants devoid of the 1,2-dihydroxy substitution (noted AH since they essentially transfer one H atom to DPPH). The corresponding radicals are expected to be less stable and either quickly recombine into inert dimers (rate constant  $k_d$ ) and/or are reactive enough to abstract the NH hydrogen atom of diphenylpicrylhydrazine (DPPHH) so that H abstraction becomes reversible (rate constants  $k_1$  and  $k'_1$  for the forward and backward reactions, respectively). Both hypotheses are required for a correct fitting of the kinetic data.

**Table 3.** Abstraction of H Atoms from Flavanol Oligomers and Dicafeoyl Esters by DPPH (MeOH, 25 °C)<sup>a</sup>

anti-oxidant	DPPH/antioxidant molar ratio (kinetic model)	$k_{1e}$ (M <sup>-1</sup> s <sup>-1</sup> ) or $k_1$	$k_{1i}$ (M <sup>-1</sup> s <sup>-1</sup> )	$k_2$ (M <sup>-1</sup> s <sup>-1</sup> )	$n$
PdB3	8 (3)	3134 ± 246	966 ± 32	30 ± 10	
	8 (1)	2950 ± 200			4.40 ± 0.03
	11.4 (3)	3316 ± 336	1118 ± 162	48 ± 10	
	11.4 (1)	3610 ± 261			4.55 ± 0.22
PB3	8 (3)	1179 ± 10	207 ± 14	57 ± 1	
	8 (1)	924 ± 14			4.55 ± 0.07
	11.4 (3)	923 ± 84	227 ± 8	48 ± 2	
	11.4 (1)	836 ± 47			4.74 ± 0.04
PC2	16 (3)	981 ± 32	236 ± 18	51 ± 4	
	16 (1)	825 ± 47			4.83 ± 0.10
	8 (3)	1442 ± 27	158 ± 1	15 ± 0	
	8 (1)	1112 ± 10			5.01 ± 0.02
cynarin	11.4 (3)	1403 ± 25	160 ± 19	16 ± 3	
	11.4 (1)	1024 ± 75			5.37 ± 0.32
	16 (3)	1497 ± 261	145 ± 5	26 ± 3	
	16 (1)	910 ± 34			5.78 ± 0.05
DCQA1	5.7 (3)	372 ± 13	69 ± 2	12 ± 1	
	5.7 (1)	365 ± 5			3.75 ± 0.02
	8 (3)	418 ± 3	109 ± 1	5 ± 1	
	8 (1)	433 ± 6			3.90 ± 0.05
DCQA2	11.4 (3)	599 ± 14	192 ± 7	7 ± 1	
	11.4 (1)	659 ± 19			4.03 ± 0.04
	5.7 (3)	700 ± 26	91 ± 1	21 ± 3	
	5.7 (1)	698 ± 2			3.29 ± 0.01
DCQA2	8 (3)	913 ± 34	149 ± 12	12 ± 3	
	8 (1)	916 ± 54			3.31 ± 0.07
	11.4 (3)	1044 ± 77	147 ± 8		
	11.4 (1)	1360 ± 60			3.25 ± 0.06
DCQA2	5.7 (3)	803 ± 49	59 ± 19	16 ± 6	
	5.7 (1)	752 ± 20			2.89 ± 0.04
	8 (3)	881 ± 5	100 ± 7		
	8 (1)	912 ± 77			2.94 ± 0.05
DCQA2	11.4 (3)	1079 ± 15	71 ± 5		
	11.4 (1)	1231 ± 23			2.74 ± 0.01

<sup>a</sup> Rate constants calculated from the curve-fitting of the absorbance (515 nm) vs time plots according to model 1 ( $k_1$ ,  $n$ ) or model 3 ( $k_{1e}$ ,  $k_{1i}$ ,  $k_2$ ). For details, see text. DCTA, slow decay, no valid kinetic model.

The rate law for AH and DPPH and the steady-state hypothesis for A are expressed as eqs 12 and 13, respectively. Solving eq 13 for [A] and using that in eq 12 gives eq 14, which

$$-\frac{d}{dt}[\text{AH}] = -\frac{d}{dt}[\text{DPPH}] = k_1[\text{AH}][\text{DPPH}] - k'_1[\text{A}][\text{DPPHH}] \quad (12)$$

$$\frac{d}{dt}[\text{A}] = 0 = k_1[\text{AH}][\text{DPPH}] - k'_1[\text{A}][\text{DPPHH}] - 2k_d[\text{A}]^2 \quad (13)$$

was used in the curve-fitting procedure,  $k_1$  and  $k = k'_1/(4k_d)$  being the *floating* parameters.

$$-\frac{d}{dt}[\text{AH}] = -\frac{d}{dt}[\text{DPPH}] = k_1[\text{AH}][\text{DPPH}] - k(A_0/\epsilon - [\text{DPPH}])^2 \times \left( \sqrt{1 + \frac{2k_1}{k} \frac{[\text{AH}][\text{DPPH}]}{(A_0/\epsilon - [\text{DPPH}])^2}} - 1 \right) \quad (14)$$

Although  $k$  turned out to be rather sensitive to the DPPH–antioxidant molar ratio,  $k_1$  values in fair agreement were found

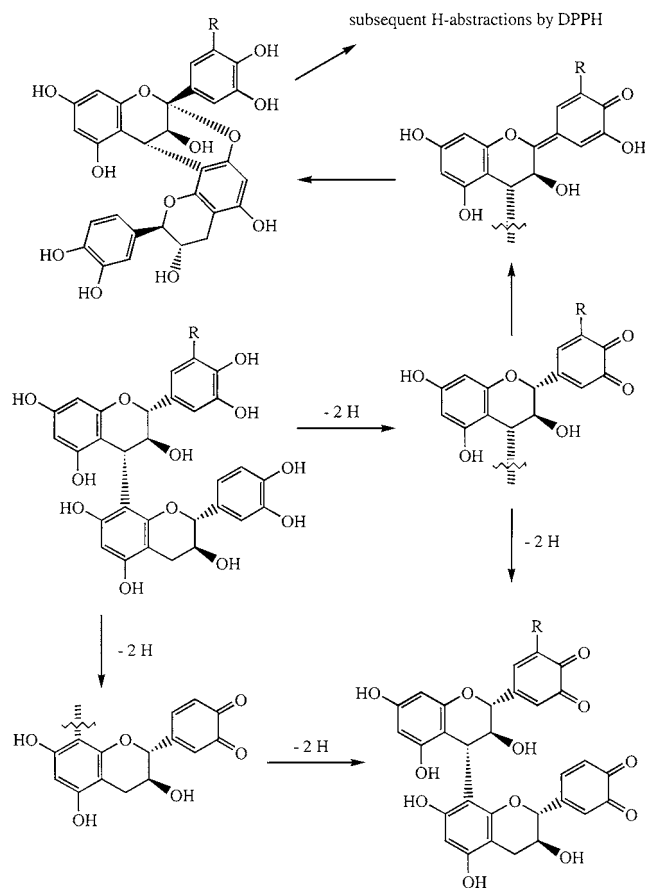


Figure 4. Proposed pathways of oxidative degradation of procyanidin dimers during radical capture [adapted from ref (47)].

Table 4. Abstraction of H Atoms from Flavonols by DPPH (MeOH, 25 °C)<sup>a</sup>

anti-oxidant	DPPH/antioxidant unit molar ratio	$k_1$ ( $M^{-1} s^{-1}$ )	$k$ ( $M^{-1} s^{-1}$ )
QG	3.2	614 ± 55	548 ± 163
	4	558 ± 18	224 ± 97
	5.7	580 ± 7	255 ± 25
IG	3.2	2850 ± 579	64 ± 33
	4	3042 ± 310	84 ± 38

<sup>a</sup> Rate constants calculated from the curve-fitting of the absorbance (515 nm) vs time plots according to model 4. For details, see text. QDG, very slow decay, no valid kinetic model.

along the different runs (Table 4). They are assumed to reasonably reflect the rate of H abstraction.

In the flavonol series, the dependence of the  $k_1$  value on the antioxidant structure suggests that H atom abstraction preferentially takes place according to the following sequence: C(4')-OH > C(3)-OH > C(3')-OH. Hence, despite its low stoichiometry, IG readily transfers the labile H atom from C(3)-OH before being converted into inert dimers.

## CONCLUSION

The H-atom-donating capacity of polyphenols is an important biologically significant property, in line with the ability of these plant antioxidants to convert potentially damaging ROS (oxyl and peroxy radicals) into nontoxic species. As a first approach, the H-atom-donating capacity of polyphenols can be conveniently and quantitatively assessed from the stoichiometry and the kinetics of their reaction with DPPH. Although the overall

mechanism is clearly complex, as evidenced by the high total stoichiometries ( $n_{tot} = 2-5$ ) typically measured with polyphenols having a 1,2-dihydroxy substitution, simple kinetic analysis readily gives access to the rate constant of the first H atom abstraction ( $k_1$ ). With antioxidants displaying more than one polyphenolic nuclei (e.g., procyanidin oligomers, dicaffeoyl esters), it is even possible to highlight differences of reactivity between these subunits. In addition, the mildly reactive DPPH radical allows a good discrimination between polyphenols, as demonstrated by the relatively large range of  $k_1$  values (ca. 400–5000  $M^{-1} s^{-1}$ ) estimated in this work. It is hoped that simple estimations of antioxidant capacities from the trapping of colored radicals (DPPH and galvinoxyl radicals, ABTS radical cation) will increasingly be aimed at rate constant determination rather than solely the determination of static parameters (stoichiometry,  $EC_{50}$ ), since a fast reaction with low concentrations of potentially damaging radicals is undoubtedly of prime importance in the antioxidant protection.

## ABBREVIATIONS USED

EGC, (+)-epigallocatechin; PdB3, prodelfphinidin B3; PC2, procyanidin C2; PB3, procyanidin B3; QG, quercetin-4'- $\beta$ -D-glucoside; QDG, quercetin-3,4'-di- $\beta$ -D-glucoside; IG, isorhamnetin-4'- $\beta$ -D-glucoside; DCTA, (*R,R*)-dicaffeoyltartaric acid; DCQA, dicaffeoylquinic acid; DPPH, 1,1-diphenyl-2-picrylhydrazyl; RP-HPLC, reverse-phase liquid chromatography; HPLC/MS, liquid chromatography coupled to mass spectrometry.

## LITERATURE CITED

- Hertog, M. G. L.; Feskens, E. J. M.; Hollman, P. C. H.; Katan, M. B.; Kromhout, D. Dietary antioxidant flavonoids and risk of coronary heart disease: the Zutphen elderly study. *Lancet* **1993**, *342*, 1007–1011.
- Hollman, P. C. H.; Katan, M. B. Dietary flavonoids: intake, health effects and bioavailability. *Food Chem. Toxicol.* **1999**, *37*, 937–942.
- Pietta, P.-G. Flavonoids as antioxidants. *J. Nat. Prod.* **2000**, *63*, 1035–1042.
- Cos, P.; Ying, L.; Calomme, M.; Hu, J. P.; Cimanga, K.; Van Poel, B.; Pieters, L.; Vlietinck, A. J.; Vanden Berghe, D. Structure–activity relationship and classification of flavonoids as inhibitors of xanthine oxidase and superoxide scavengers. *J. Nat. Prod.* **1998**, *61*, 71–76.
- Foti, M.; Piattelli, M.; Baratta, M. T.; Ruberto, G. Flavonoids, coumarins, and cinnamic acids as antioxidants in a micellar system. Structure–activity relationship. *J. Agric. Food Chem.* **1996**, *44*, 497–501.
- Dangles, O.; Dufour, C.; Fargeix, G. Inhibition of lipid peroxidation by quercetin and quercetin derivatives: antioxidant and prooxidant effects. *J. Chem. Soc., Perkin Trans. 2* **2000**, 1215–1222.
- Jovanovic, S. V.; Steenken, S.; Hara, Y.; Simic, M. G. Reduction potentials of flavonoid and model phenoxyl radicals. Which ring in flavonoids is responsible for the antioxidant activity? *J. Chem. Soc., Perkin Trans. 2* **1996**, 2497–2504.
- Bors, W.; Heller, W.; Michel, C.; Saran, M. Flavonoids as antioxidants: determination of radical scavenging activities. *Methods Enzymol.* **1990**, *186*, 343–355.
- Jovanovic, S. V.; Steenken, S.; Tosic, M.; Marjanovic, B.; Simic, M. G. Flavonoids as antioxidants. *J. Am. Chem. Soc.* **1994**, *116*, 4846–4851.
- Van Acker, S. A. B. E.; Van den Berg, D.-J.; Tromp, M. N. J. L.; Griffioen, D. H.; Van der Vijgh, W. J. F.; Bast, A. Structural aspects of antioxidant activity of flavonoids. *Free Radical Biol. Med.* **1996**, *20*, 331–342.
- Rice-Evans, C.; Miller, N. J.; Paganga, G. Structure-antioxidant activity relationships of flavonoids and phenolic acids. *Free Radical Biol. Med.* **1996**, *20*, 933–956.

- (12) Vinson, J. A.; Dabbagh, Y. A.; Serry, M. M.; Jang, J. Plant flavonoids, especially tea flavanols, are powerful antioxidants using an in vitro oxidation model for heart disease. *J. Agric. Food Chem.* **1995**, *43*, 2800–2802.
- (13) Riedl, K. M.; Hagerman, A. E. Tannin–protein complexes as radical scavengers and radical sinks. *J. Agric. Food Chem.* **2001**, *49*, 4917–4923.
- (14) Cotellet, N.; Bernier, J.-L.; Catteau, J.-P.; Pommery, J.; Wallet, J.-C.; Gaydou, E. M. Antioxidant properties of hydroxyflavones. *Free Radical Biol. Med.* **1996**, *20*, 35–43.
- (15) Scalbert, A.; Williamson, G. Dietary intake and bioavailability of polyphenols. *J. Nutr.* **2000**, *130*, 2073S–2085S.
- (16) Manach, C.; Morand, C.; Crespy, V.; Demigné, C.; Texier, O.; Régéat, F.; Rémésy, C. Quercetin is recovered in human plasma as conjugated derivatives which retain antioxidant properties. *FEBS Lett.* **1998**, *426*, 331–336.
- (17) Da Silva, E.; Piskula, M. K.; Yamamoto, N.; Moon, J.-H.; Terao, J. Quercetin metabolites inhibit copper-induced lipid peroxidation in rat plasma. *FEBS Lett.* **1998**, *430*, 405–408.
- (18) Halliwell, B.; Zhao, K.; Whiteman, M. The gastrointestinal tract: a major site of antioxidant action? *Free Radical Res.* **2000**, *33*, 819–830.
- (19) Kanner, J.; Lapidot, T. The stomach as a bioreactor: dietary lipid peroxidation in the gastric fluid and the effects of plant-derived antioxidants. *Free Radical Biol. Med.* **2001**, *31*, 1388–1395.
- (20) Sanchez-Moreno, C.; Larrauri, J. A.; Saura-Calixto, F. A procedure to measure the antiradical efficiency of polyphenols. *J. Sci. Food Agric.* **1998**, *76*, 270–276.
- (21) Goupy, P.; Hugues, M.; Boivin, P.; Amiot, M. J. Antioxidant composition and activity of barley (*Hordeum vulgare*) and malt extracts and of isolated phenolic compounds. *J. Sci. Food Agric.* **1999**, *79*, 1625–1634.
- (22) Dangles, O.; Fargeix, G.; Dufour, C. One-electron oxidation of quercetin and quercetin derivatives in protic and non protic media. *J. Chem. Soc., Perkin Trans. 2* **1999**, 1387–1395.
- (23) Dangles, O.; Fargeix, G.; Dufour, C. Antioxidant properties of anthocyanins and tannins: a mechanistic investigation with catechin and the 3',4',7-trihydroxyflavylium ion. *J. Chem. Soc., Perkin Trans. 2* **2000**, 1653–1663.
- (24) Dufour, C.; da Silva, E.; Potier, P.; Queneau, Y.; Dangles, O. Gallic esters of sucrose as efficient radical scavengers in lipid peroxidation. *J. Agric. Food Chem.* **2002**, *50*, 3425–3430.
- (25) Alluis, B.; Dangles, O. Quercetin glycosides and sulfates: chemical synthesis, complexation and antioxidant properties. *Helv. Chim. Acta* **2001**, *84*, 1133–1156.
- (26) Fougerousse, A.; Gonzalez, E.; Brouillard, R. A convenient method for synthesizing 2-aryl-3-hydroxy-4-oxo-4H-1-benzopyrans or flavonols. *J. Org. Chem.* **2000**, *65*, 583–586.
- (27) Price, K. R.; Rhodes, M. J. C. Analysis of the major flavonol glycosides present in four varieties of onion (*Allium cepa*) and changes in composition resulting from autolysis. *J. Sci. Food Agric.* **1997**, *74*, 331–339.
- (28) Gil-Izquierdo, A.; Gil, M. I.; Conesa, M. A.; Ferreres, F. The effect of storage temperature on vitamin C and phenolics content of artichoke (*Cynara scolymus* L.) heads. *Innov. Food Sci., Emerg. Technol.* **2001**, *2*, 199–202.
- (29) Wöldecke, M.; Herrmann, K. D-(+)-Dicafeoyl tartaric acid from endives (*Cichorium endivia* L.). *Z. Naturforsch.* **1974**, *29c*, 360–361.
- (30) Dangles, O.; Dufour, C.; Bret, S. Flavonol-serum albumin complexation. Two-electron oxidation of flavonols and their complexes with serum albumin. *J. Chem. Soc., Perkin Trans. 2* **1999**, 737–744.
- (31) Jungbluth, G.; Rühling, I.; Ternes, W. Oxidation of flavonols with Cu(II), Fe(II) and Fe(III) in aqueous medium. *J. Chem. Soc., Perkin Trans. 2* **2000**, 1946–1952.
- (32) Utaka, M.; Takeda, A. Copper(II)-catalysed oxidation of quercetin and 3-hydroxyflavone. *J. Chem. Soc., Chem. Commun.* **1985**, 1824–1826.
- (33) Smith, M. A.; Webb, R. A.; Cline, L. J. The oxidation of flavonols by periodic acid in methanol. *J. Org. Chem.* **1965**, *30*, 995–997.
- (34) Jorgensen, L. V.; Cornett, C.; Justesen, U.; Skibsted, L. H.; Dragsted, L. O. Two-electron electrochemical oxidation of quercetin and kaempferol changes only the flavonoid C-ring. *Free Radical Res.* **1998**, *29*, 339–350.
- (35) Igarashi, K.; Komatsu, C.; Shimada, T. 2,5,7,3',4'-Pentahydroxyflavan-3,4-dione as an intermediate product in the enzyme-catalysed oxidation of quercetin. *Agric. Biol. Chem.* **1991**, *55*, 855–857.
- (36) Fulcrand, H.; Cheminat, A.; Brouillard, R.; Cheynier, V. Characterization of compounds obtained by chemical oxidation of caffeic acid in acidic conditions. *Phytochemistry* **1994**, *35*, 499–505.
- (37) Hapiot, P.; Neudeck, A.; Pinson, J.; Fulcrand, H.; Neta, P.; Rolando, C. Oxidation of caffeic acid and related hydroxycinnamic acid. *J. Electroanal. Chem.* **1996**, *405*, 169–176.
- (38) Plumb, G. W.; De Pascual-Teresa, S.; Santos-Buelga, C.; Cheynier, V.; Williamson, G. Antioxidant properties of catechins and proanthocyanidins: effect of polymerisation, galloylation and glycosylation. *Free Radical Res.* **1998**, *29*, 351–358.
- (39) Young D. A.; Young, E.; Roux, D. G.; Brandt, V.; Ferreira, D. Synthesis of condensed tannins. Part 19. Phenol oxidative coupling of (+)-catechin and (+)-mesquitol. Conformation of bis-(+)-catechins. *J. Chem. Soc., Perkin Trans. 1* **1987**, 2345–2351.
- (40) Guyot, S.; Vercauteren, J.; Cheynier, V. Structural determination of colourless and yellow dimers resulting from (+)-catechin coupling catalysed by grape polyphenoloxidase. *Phytochemistry* **1996**, *42*, 1279–1288.
- (41) Kondo, K.; Kurihara, M.; Fukuhara, K.; Tanaka, T.; Suzuki, T.; Miyata, N.; Toyoda, M. Conversion of procyanidin B-type (catechin dimer) to A-type: evidence for abstraction of C-2 hydrogen in catechin during radical oxidation. *Tetrahedron Lett.* **2000**, *41*, 485–488.
- (42) Bors, W.; Michel, C.; Stettmaier, K. Electron paramagnetic resonance studies of radical species of proanthocyanidins and gallate esters. *Arch. Biochem. Biophys.* **2000**, *374*, 347–355.
- (43) Horman, I.; Badoud, R.; Ammann, W. Food-related applications of one- and two-dimensional high-resolution proton nuclear magnetic resonance: structure and conformation of cynarin. *J. Agric. Food Chem.* **1984**, *32*, 538–540.

---

Received for review September 5, 2002. Revised manuscript received November 14, 2002. Accepted November 18, 2002.

JF025938L